Computational Brain & Behavior
https://doi.org/10.1007/s42113-023-00191-4

ORIGINAL PAPER

Bayesian Graphical Modeling with the Circular Drift Diffusion Model

Manuel Villarreal[1] · Adriana F. Chávez De la Peña[1] · Percy K. Mistry[2] · Vinod Menon[2,3,4] · Joachim Vandekerckhove[1] · Michael D. Lee[1]

Accepted: 3 November 2023
© Society for Mathematical Psychology 2023

Abstract
The circular drift-diffusion model (CDDM) is a sequential sampling model designed to account for decisions and response times in decision-making tasks with a circular set of choice alternatives. We present and demonstrate a fully Bayesian implementation and extension of the CDDM. This development allows researchers to apply the CDDM to data from complex experiments and draw conclusions about targeted hypotheses. The Bayesian implementation relies on a custom JAGS module. We describe the module and demonstrate its adequacy through a simulation study. We then illustrate the advantages of the implementation by revisiting data from a continuous orientation judgment task. We develop a graphical model for the analysis that is based on the CDDM but extends it with hierarchical and latent-mixture structures. We then demonstrate how these extensions are used to accommodate the design of the experiment and to implement psychological assumptions about individual differences, the difficulty of different stimulus conditions, and the impact of cues on decision making. Finally, we demonstrate how the computational Bayesian inference enabled by JAGS allows these assumptions to be tested and addresses psychological research questions about people's decision making.

Keywords Circular drift diffusion model · JAGS · Hierarchical model · Latent-mixture models · Bayesian inference

Introduction

The circular drift-diffusion model (CDDM; Smith, 2016) is a sequential sampling decision model that extends the widely used drift-diffusion model (DDM; Ratcliff, 1978; Ratcliff & McKoon, 2008) to the circular domain. In the classical DDM, it is assumed that evidence from a stimulus is repeatedly sampled until a boundary is reached, at which point the decision associated with that boundary is made. The model makes predictions about both the decisions people make and the time they take to make them. The DDM is designed for tasks with discrete decisions and is most often applied to two-choice tasks.

The CDDM considers situations in which the boundary of evidence accumulation is an encompassing circle. This extension implies that there exists a continuum of possible decisions, corresponding to points on the circle and that there is a similarity relationship between the decision alternatives. The CDDM has been applied in other decision settings including targets presented in visual displays (Smith & Corbett, 2019), the orientation of line segments (Kvam, 2019), color identification by eye movement (Smith et al., 2020), color-coded contexts in source-memory retrieval tasks (Zhou et al., 2021), and spatial location coded contexts in lexical memory tasks (Zhou et al., 2023). Figure 1 provides examples of three more possibilities: choosing a color from a wheel to identify the color of a shirt, choosing the spatial direction of a voice, and choosing a time in a calendar year.

In this article, we introduce a custom JAGS module that implements the CDDM. JAGS is a high-level scripting language for implementing probabilistic generative models and automating Bayesian inference using computational sampling methods (Plummer, 2003). JAGS is widely used to develop, evaluate, and apply cognitive models (Lee &

✉ Michael D. Lee
mdlee@uci.edu

1 Department of Cognitive Sciences, University of California Irvine, Irvine, CA 92697-5100, USA

2 Department of Psychiatry and Behavioral Sciences, Stanford University School of Medicine, Stanford, USA

3 Department of Neurology and Neurological Sciences, Stanford University School of Medicine, Stanford, USA

4 Wu Tsai Stanford Neuroscience Institute, Stanford University School of Medicine, Stanford, USA

Published online: 04 December 2023

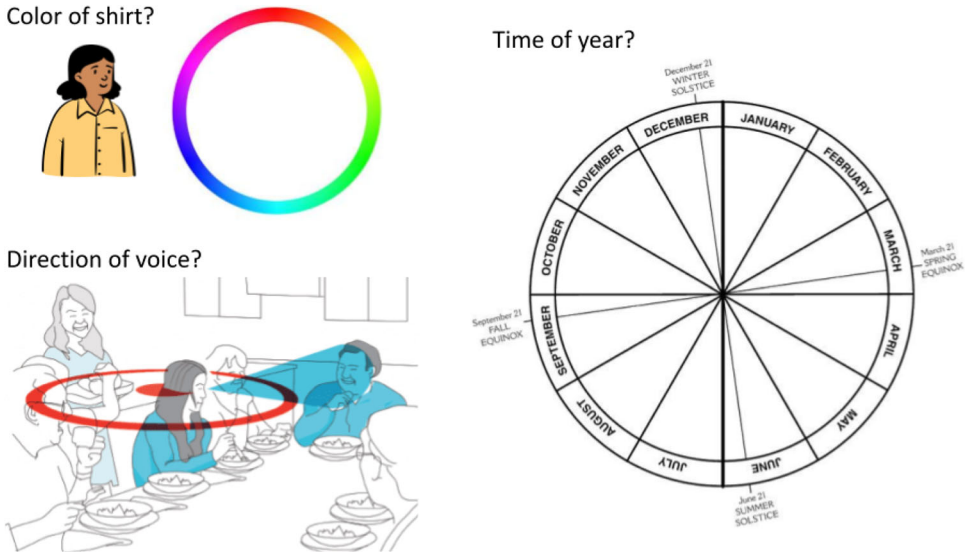

Fig. 1 Examples of circular decisions. The top left panel shows a hue identification task where the color of the shirt has to be located along the color wheel. The bottom left panel illustrates a situation in which a person must spatially locate the source of a relevant auditory stimulus (e.g., a voice). The right panel presents the decision space for questions about the occurrence of an event of interest during the calendar year

Wagenmakers, 2013). There are at least two reasons to develop custom modules. The first, as demonstrated by Wabersich & Vandekerckhove (2014) for the DDM, is that it makes non-standard statistical distributions available. Sometimes, when a new distribution is composed of combinations of standard distributions, this is just a matter of convenience. Other times, when the probability density function of the new distribution relies on procedural calculations that are not part of the base JAGS language, a module is needed to make it available at all. The second advantage of custom modules, as argued by Lee (2011, 2018), is that they facilitate the development of tailored graphical models. In particular, JAGS makes it easy to construct hierarchical, latent mixture, and common cause models in order to capture the context in which behavioral data are observed and to allow models to answer specific research questions.

The structure of this article is as follows. We begin by providing a statistical specification of the CDDM. We then implement the CDDM in JAGS and present the results of a parameter recovery study that demonstrates the accuracy of our implementation. To illustrate the use of the module, we present an application to data collected in a continuous orientation judgment task by Kvam (2019). Our application is based on a graphical model that extends the CDDM with hierarchical and latent-mixture structures. These extensions allow the model to accommodate the design of the experiment and to implement psychological assumptions about individual differences, the difficulty of different stimulus conditions, and the impact of cues on decision making. We demonstrate how the computational Bayesian inference enabled by JAGS allows these assumptions to be tested and addresses psychological research questions about people's decision making. We conclude with a discussion of possible applications of the CDDM within JAGS, including potential extensions to decision tasks in which the circular continuum is partitioned into a set of structured discrete choice alternatives.

The Circular Drift Diffusion Model

The CDDM, shown in Fig. 2, assumes that evidence for a decision begins at the origin of a circle and is accumulated sequentially in time until the evidence tally reaches the circumference. Evidence accumulation is represented as a two-dimensional random walk, such that the evidence state $\boldsymbol{s}_t$ at any point in time t can be described using Cartesian coordinates $\boldsymbol{s}_t = (x_t, y_t)$, or the corresponding polar coordinates m_t and d_t, where m_t is the radial distance from the origin and $0 \leq d_t < 2\pi$ is the angular orientation in radians. Once the evidence accumulation reaches the circumference, the corresponding decision alternative is selected. The result of this process on each trial is a two-dimensional outcome containing the angle of the alternative selected in radians and the associated response time.

The CDDM requires at least four parameters to describe the response process. The non-decision time $\tau \geq 0$ is the fixed amount of time that participants take to encode stimulus information and execute a motor response. The boundary radius $\eta > 0$ determines the amount of evidence required before committing to a decision. The drift angle $0 \leq \theta \leq 2\pi$ represents the angular direction in radians of the decision alternative favored by the stimulus presented. Finally, the drift length $\delta > 0$ indicates the speed with which the participant accumulates information towards the decision implied by the drift angle θ.

Together, the drift angle θ and drift length δ describe the information provided by the stimulus and its effect on the

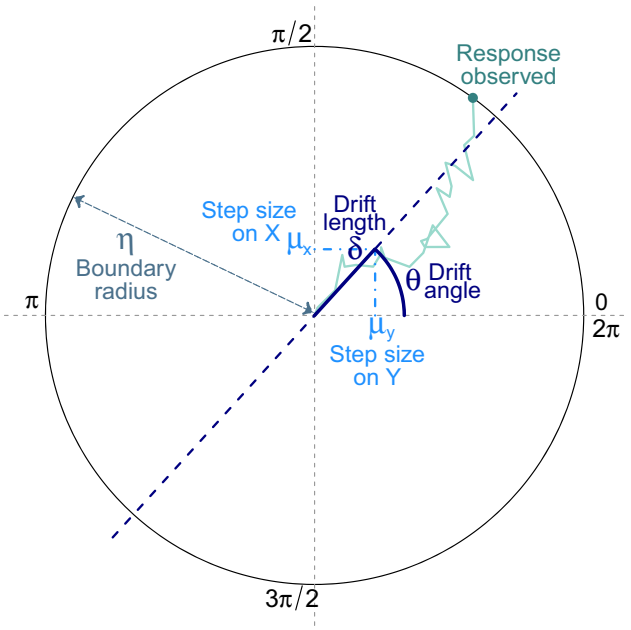

Fig. 2 In the CDDM, the evidence accumulation process is a two-dimensional random walk from the origin of a circle to its circumference. The boundary radius η determines the amount of evidence required before committing to an answer. The drift vector $\boldsymbol{\mu} = (\mu_x, \mu_y)$ specifies the mean step size on the x and y coordinates. The drift vector can also be expressed in polar coordinates, with the drift angle θ and drift length δ indicating the average direction and speed of the random walk. The non-decision time parameter τ is not depicted

speed and direction of the evidence accumulation process. The drift angle θ and drift length δ correspond to the polar coordinates of the drift vector $\boldsymbol{\mu} = (\mu_x, \mu_y)$ that specifies the mean step size of the random walk process on the x and y dimension, respectively, in Cartesian coordinates. Translating between these two coordinate systems is straightforward using the following system of equations:

$$\begin{aligned} \delta &= \sqrt{\mu_x^2 + \mu_y^2} \\ \theta &= \arctan\left(\frac{\mu_y}{\mu_x}\right) \\ (\mu_x, \mu_y) &= (\delta\cos(\theta), \delta\sin(\theta)). \end{aligned} \tag{1}$$

Much like in other sequential sampling models, the non-decision time and boundary radius are assumed to be fixed across trials while the drift parameters describing the information provided by the stimuli are assumed to vary. At any given moment in time t, the evidence accumulated along the x and y axes $\boldsymbol{s}_t = (x_t, y_t)$ is assumed to be independent and identically distributed, such that $x_t \sim \text{Gaussian}(\mu_x, \sigma^2)$ and $y_t \sim \text{Gaussian}(\mu_y, \sigma^2)$.

The CDDM Likelihood Function

An attractive property of the CDDM is that the implied distribution of data given parameters is computationally tractable. The bivariate probability density function, which expresses the joint probability density of decision c and reaction time t, is given by (Qarehdaghi & Rad, 2022; Smith, 2016):

$$\begin{aligned} p(c, t \mid \delta, \theta, \eta, \tau) = {} & \frac{\sigma^2}{2\pi\eta^2}\exp\left(-\frac{1}{2\sigma^2}\left[\delta^2(t-\tau) - 2\eta\delta\cos(c-\theta)\right]\right) \\ & \times \sum_{k=1}^{+\infty}\left[\frac{j_{0,k}}{J_1(j_{0,k})}\exp\left(-\frac{1}{2\eta^2}(t-\tau)j_{0,k}^2\sigma^2\right)\right] \\ \Leftrightarrow (c, t) \sim {} & \text{CDDM}_\circ(\delta, \theta, \eta, \tau), \end{aligned} \tag{2}$$

or equivalently in Cartesian coordinates:

$$\begin{aligned} p(c, t \mid \mu_x, \mu_y, \eta, \tau) = {} & \frac{\sigma^2}{2\pi\eta^2}\exp\Big(-\frac{1}{2\sigma^2}\Big[\left(\mu_x^2 + \mu_y^2\right)(t-\tau) \\ & -2\eta(\mu_x\cos(c) + \mu_y\sin(c))\Big]\Big) \\ & \times \sum_{k=1}^{+\infty}\left[\frac{j_{0,k}}{J_1(j_{0,k})}\exp\left(-\frac{1}{2\eta^2}(t-\tau)j_{0,k}^2\sigma^2\right)\right] \\ \Leftrightarrow (c, t) \sim {} & \text{CDDM}_+(\mu_x, \mu_y, \eta, \tau). \end{aligned} \tag{3}$$

Throughout, we will choose $\sigma = 1$ to identify the model. In these two functions, $J_1()$ and $j_{0,k}$ are, respectively, a first-order Bessel function of the first kind and the k^{th} zero of a zero-order Bessel function.

The left panel of Fig. 3 provides an illustration of the CDDM. A number of evidence accumulation paths from the origin to the circumference are shown, and the shading along the circumference shows the resulting distribution of decisions. This marginal distribution of decisions is shown again in the top right panel and the marginal distribution of response times is shown in the bottom right panel.

JAGS Implementation of the CDDM

Custom Module

The steps to constructing a custom JAGS module are laid out in Wabersich & Vandekerckhove (2014). The process has become more efficient since the publication of that tutorial, in that there now exist a number of repositories[1] with example modules that can be used as a starting point, and in particular the **jags-moduleTemplate** repository https://github.com/

[1] Some examples are **jags-wiener** (Wabersich, 2018), **jags-vonmises** (Wabersich, 2016b), **jags-amoroso** (Wabersich, 2016a), **jags-exgauss** (Selker, 2016), and **jags-rescorlaWagner** (Selker, 2018b).

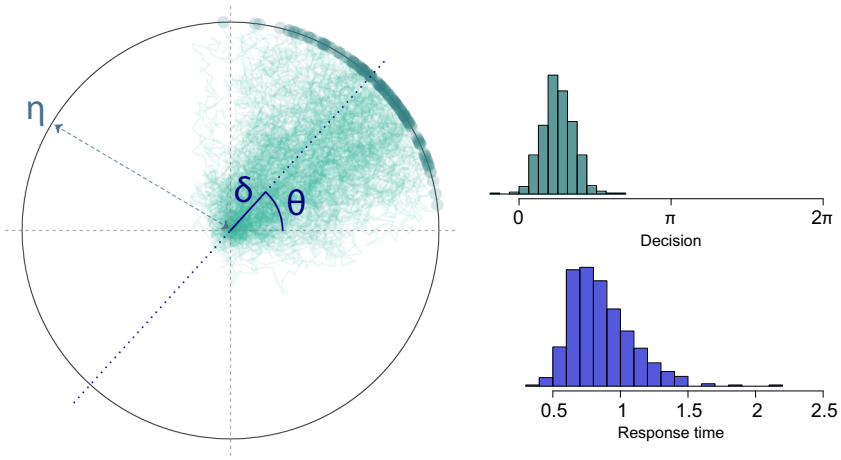

Fig. 3 An illustration of the distribution of decision and response times predicted by the CDDM. The left panel shows different random walks observed over 100 trials, with the shaded points along the circumference indicating the decisions registered every time. All random walks present a decision process with the same boundary radius, non-decision time, and drift vector parameters. The top right panel shows the observed distribution of decisions in radians. The bottom right panel shows the positively-skewed observed distribution of response times

raviselker/jags-moduleTemplate/ by Selker (2018a). With these resources, the remaining effort in creating a JAGS module is in the writing of applicable `logDensity` functions and a handful of housekeeping functions such as `typicalValue` and `checkParameterValue`. Because the CDDM likelihood is vector-valued (i.e., the model applies to bivariate data), the module defines `VectorDist` (vector-valued distribution) objects with length 2.

The module[2] can be obtained via https://github.com/joachimvandekerckhove/jags-cddm/. The core code for the density function evaluation can be found in `src/distributions/DCDDM.cc`. That file implements the logarithm of the Cartesian formulation of the likelihood given in Eq. 3:

$$\begin{aligned}\ell\left(c,t \mid \mu_x,\mu_y,\eta,\tau\right) \approx & -\log\left(2\pi\eta^2\right) - \frac{t-\tau}{2}\left(\mu_x^2+\mu_y^2\right) \\ & +\eta(\mu_x\cos(c)+\mu_y\sin(c)) \\ & +\log\left(\sum_{k=1}^{50}\left[\frac{j_{0,k}}{J_1(j_{0,k})}\exp\left(-\frac{t-\tau}{2}\frac{j_{0,k}^2}{\eta^2}\right)\right]\right). \quad (4)\end{aligned}$$

The polar version of the likelihood is implemented by transforming the input parameters using System 1 and then calculating Eq. 4. Note that $j_{0,k}/J_1\left(j_{0,k}\right)$ and $j_{0,k}^2$ are only a function of the summation counter k and not of any of the function's parameters or variables, so they can be precomputed for speed. We approximate the infinite sum by computing only the first 50 terms, which we have found to be sufficient – the contribution of the 50$^{\text{th}}$ term is less than 0.1% of the total sum as long as the scaled time factor $(t-\tau)/\eta^2$ is at least 0.004. In the small-t range, Eq. 4 becomes numerically unstable when $\sqrt{\mu_x^2+\mu_y^2}$ and η are large, which can impede parameter estimation. Smith et al. (2023) demonstrate with values of $\sqrt{\mu_x^2+\mu_y^2}=5$ and $\eta=4$ and propose an updated solution to the density function. At the time of writing, this update is being implemented and tested (see the "Ongoing Work" section, below).

[2] For computational reproducibility, the GitHub repository also includes instructions for setting up a virtual machine—a curated computational environment—that includes an operating system with appropriate compilers and software versions that support the module.

Usage

The `README.md` file of the repository provides installation instructions. Once the module is installed, it can be loaded in JAGS with `load cddm`. Loading the module will enable two new distributions with the following templates. For CDDM$_\circ$():

```
X[1:2,i] ~ dcddmpolar(driftLength, driftAngle, bound, nondecision)
```

and for CDDM$_+$():

```
X[1:2,i] ~ dcddmcartn(driftx, drifty, bound, nondecision)
```

In both cases, `X[1,i]` is the decision in radians, and `X[2,i]` is the reaction time in seconds. `dcddmpolar()` takes the parameters expressed in polar terms $(\delta,\theta,\eta,\tau)$ and `dcddmcartn()` takes the parameters expressed in Cartesian terms (μ_x,μ_y,η,τ). All input parameters are scalars.

The θ parameter exists in a circular domain, which somewhat complicates the MCMC sampling, especially if its posterior distribution has significant mass near the edge of the (arbitrarily chosen) 2π-interval over which it is defined. While these complications are not insurmountable, we generally prefer the Cartesian implementation.

Parameter Recovery Study

We tested the accuracy of the CDDM module in simulation studies that examined separately the parameter recovery of the Cartesian and polar coordinates implementations of

the module. We selected a small number of values for every parameter in the model and used them to simulate 200 independent data sets for every possible parameter combination. We then applied the JAGS module and compared the parameter values retrieved to those used to generate the data sets. Parameter recovery was evaluated using the distribution of the mean posteriors obtained across every data set generated using every parameter value. The recovery study does not assess the CDDM model itself, nor does it allow us to evaluate the effectiveness of the Bayesian statistical methods used to make inferences. Rather, the recovery study provides a method for checking the correctness of the implementation of the JAGS module, and for understanding the informativeness of experimental designs with respect to the CDDM and its parameters.

We used three different values of boundary radius $\eta \in (1.5, 2.0, 2.5)$ and non-decision time $\tau \in (0.1, 0.2, 0.3)$. For the recovery study testing the polar coordinate implementation of the module, we used three different values of drift angle $\theta \in (0.0, 2.0, 4.0)$ and drift length $\delta \in (0.01, 1.0, 2.0)$, while for Cartesian coordinate implementation we used four mean step size levels on the x and y coordinates, $\mu_x \in (-0.5, 0, 0.5, 1)$ and $\mu_y \in (-1, -0.5, 0, 0.5)$. Altogether, this resulted in 81 different parameter combinations in the polar implementation and 144 parameter combinations in the Cartesian implementation.

Posterior estimates were computed across four chains with 2500 recorded samples each after 500 discarded burn-in samples. All chains converged, using $\hat{R} < 1.05$ as a criterion (Gelman et al., 2013). Note that chain convergence for the drift angle θ parameter in the polar implementation was evaluated after having transformed the posterior samples into the constrained interval $0 \leq \theta < 2\pi$. This transformation was conducted using modular algebra.

The results of the parameter recovery studies are shown in Figs. 4 and 5 for the Cartesian and the polar coordinate implementations of the module, respectively. In these figures, each panel presents the distribution of the posterior means obtained across all data sets that shared the same true value of that parameter (regardless of the values of the other parameters).[3] Overall, parameters are recovered well: there are no systematic errors from the "true" parameter values used to generate the data, and the variability around these values is acceptably small with sample size 200. These results provide confirmation that the CDDM probability density functions in our JAGS module are correctly implemented.

[3] The bottom right panel of Fig. 5 excludes cases where the drift length δ true value was close to 0 (i.e., $\delta = 0.01$), as the drift angle is unidentified in that case.

Ongoing Work

The **jags-cddm** module continues to be developed. New additions will be made publicly available via the GitHub repository. The planned additions include (1) updating the likelihood function for computational stability for extreme parameter values (Smith et al., 2023), (2) adding one or more additional distribution functions for integrated cross-trial variability (Zhou et al., 2021, 2023), and (3) including an efficient and robust random number generator.

Application to Modeling Orientation Judgments

Kvam (2019) Experiment

Kvam (2019) considered a task in which participants estimated the mean orientation of a sequence of rapidly presented Gabor patches. The design of the task is summarized in Fig. 6. Trials were divided into four main blocks with two independent factors: speed versus accuracy instructions and cued versus uncued conditions. For speed trials, participants gained more points for responses made within 800ms of stimulus onset, while for accuracy trials participants earned more points the closer their estimates were to the true mean. Participants were told at the beginning of each block whether they were a part of the speed or accuracy condition, and they were also reminded of the condition with the words "SPEED" or "ACCURACY" at the beginning of each trial.

Once a trial started, participants were shown either a green line with a fixed orientation (cued condition) or a green circle at the center of the screen (uncued condition). Following the presentation of the line or circle, participants were shown a rapid sequence of Gabor patches, drawn every 16.7 ms at 60 hz, with orientations varying according to a Gaussian distribution centered at the true mean orientation with a fixed standard deviation. The standard deviations of the distribution of the samples were used to set three difficulty conditions—low, medium, and high—with standard deviations of 15, 30, and 45°, respectively. A cue could have a deflection of 0, 20, 50, or 70° in a clockwise or counterclockwise direction from the true mean orientation of the Gabor patches.

Participants could respond at any point during the presentation of the sequence of patches by moving their mouse to the edge of a response circle on the screen. The point at which they reached the edge defined their decision for the trial.

To simplify the presentation of modeling results, we consider only six of the twelve participants, chosen to be representative of the overall range of individual differences.

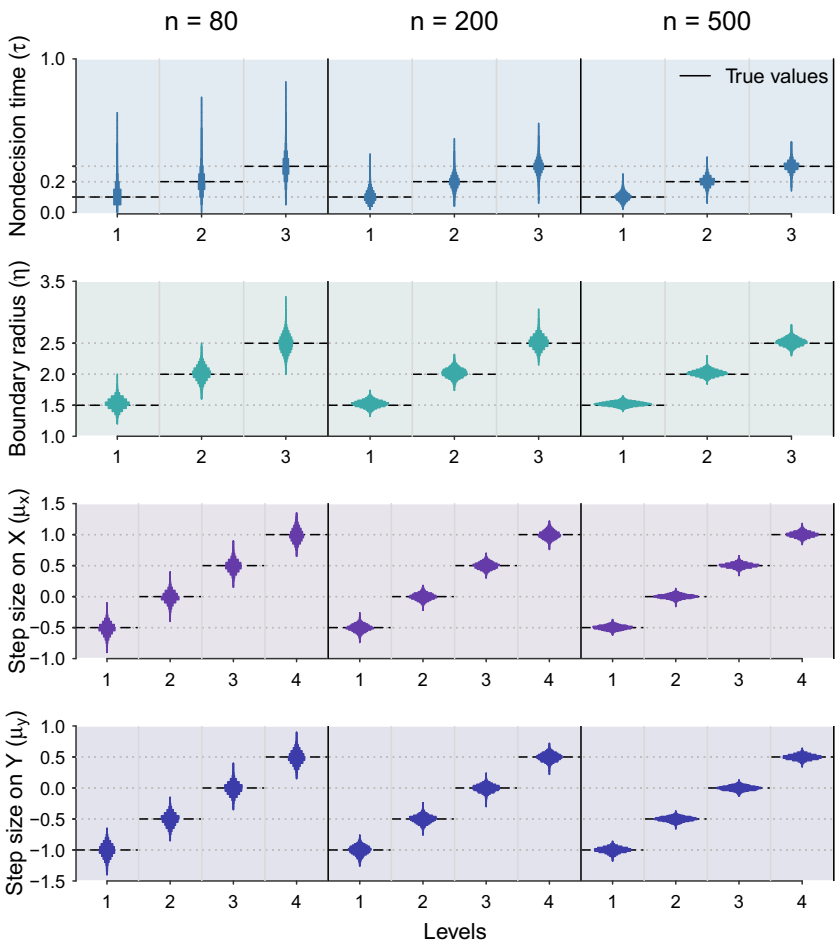

Fig. 4 Results of the parameter recovery study conducted using our Cartesian coordinate implementation of the CDDM. Every panel shows the distributions of posterior means obtained across data sets generated using each parameter value. All panels present the results obtained across three simulation studies that considered a sample size of $n = 80$, $n = 200$, and $n = 500$, respectively. The black dashed lines indicate the true values

We also only use the cued condition, since modeling the potential influence of a cue allows us to highlight some of the features of implementing the CDDM within JAGS.

Research Questions

We address four research questions related to the Kvam (2019) experiment. These research questions were not chosen because they are the most important ones in terms of understanding human perceptual decision making. Instead, they were chosen to demonstrate the flexibility of graphical models to formalize assumptions about psychological processes, and the usefulness of Bayesian methods to answer research questions.

The first research question is whether participants are more cautious when they are instructed to prioritize accuracy over speed. Statistically, this involves testing whether the boundary radius for a participant is the same or different in the speed versus accuracy conditions. The second research question is whether the speed of information processing decreases as the variability of the Gabor stimuli increases and the task becomes more difficult. Statistically, this involves testing whether the drift length satisfies an order constraint by decreasing monotonically with task difficulty. The third research question is whether participants sample information less consistently as the task becomes more difficult. This involves testing whether the variability of the drift angle satisfies an order constraint by increasing monotonically with task difficulty.

The final research question is less standard than the first three and requires the most elaborate modeling. It asks whether positive and negative deflections of cues have different impacts on participants' decision making. In particular, it considers the possibility that, on each trial, a participant could use either the cue or the Gabor stimuli as the basis for their orientation judgment. Addressing this question involves testing whether the base rate with which each source of information is used is the same or different for cue deflections of the same magnitude but in different directions. Our main motivation with this research question is that it seems likely the base rates will be the same. This allows us to consider the ability of Bayesian inference to find evidence for sameness,

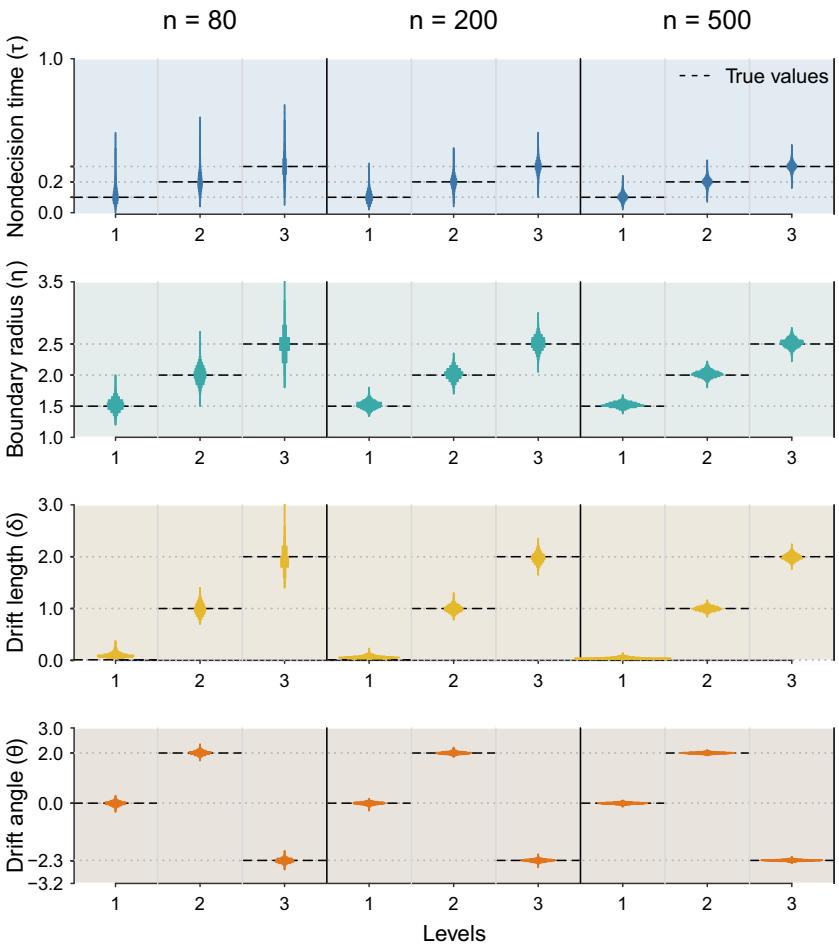

Fig. 5 Results of the parameter recovery study conducted using our polar coordinate implementation of the CDDM. Every panel shows the distributions of posterior means obtained across data sets generated using each parameter value. All panels present the results obtained across three simulation studies that considered a sample size of $n = 80$, $n = 200$, and $n = 500$, respectively. The black dashed lines indicate the true values. Note that the drift angle parameter becomes undefined as the drift length approaches 0, so the lower right panel excludes all results from the $\delta = 0.01$ condition

indicating equivalence or invariance, rather than just the ability to find evidence for differences, indicating the presence of effects.

Graphical Model

Figure 7 shows the graphical model we developed for this analysis. The decision and RT data are represented by the y_{isdct} node at the center of the model. This node is shaded and circular because the data are observed and continuous. It is at the intersection of encompassing plates for trial t of participant i with cue deflection c in speed-accuracy condition s and difficulty condition d.

$$y_{iscdt} \sim \text{CDDM}_{\circ}\left(\delta_{id}, \text{mod}(\theta_{isdct}, 2\pi), \eta_{id}, \tau_i\right) \tag{5}$$

The four CDDM parameters—drift angle, drift length, boundary radius, and nondecision time—are represented by the four nodes that are the parents of the y_{isdct} node. These nodes have different colors, and other nodes in the graphical model associated with each parameter share the same color. This helps visually parse the graphical model into the assumptions it makes about drift angle, drift length, bound-

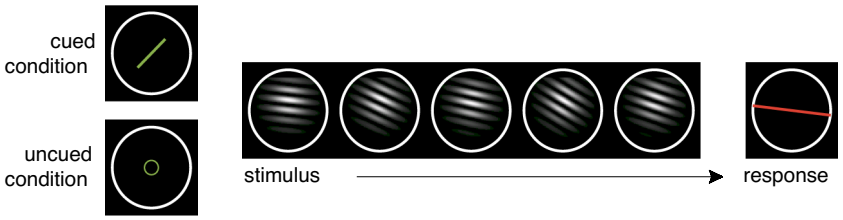

Fig. 6 The design of a trial in the orientation judgment task considered by Kvam (2019). After either being cued by a line or not being cued, a sequence of Gabor patches with a mean orientation was presented. Participants could respond at any time to indicate the mean orientation. Based on Kvam, (2019 Fig. 2)

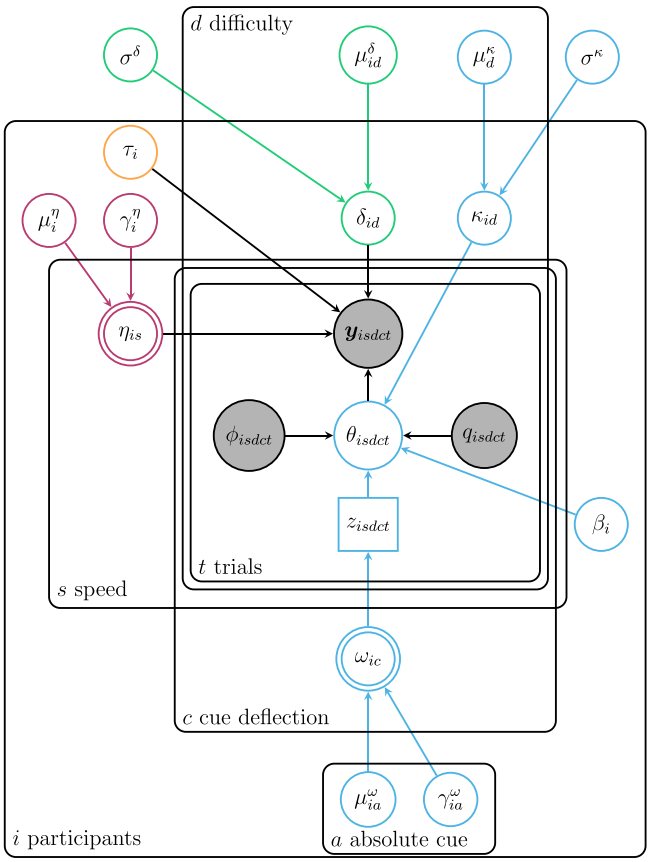

$$
\begin{aligned}
\mu_i^\eta &\sim \text{Gaussian}(0,1)\\
\gamma_i^\eta &\sim \text{Gaussian}(0,1)T(0,\infty)\\
\eta_{is} &= \begin{cases} \exp\left(\mu_i^\eta + \gamma_i^\eta/2\right) & \text{if } s = \text{accuracy}\\ \exp\left(\mu_i^\eta - \gamma_i^\eta/2\right) & \text{if } s = \text{speed}\end{cases}\\
\tau_i &\sim \text{uniform}(0, \min y_{i1})\\
\mu_d^\delta &\sim \text{Gaussian}(0,1)\\
\sigma^\delta &\sim \text{uniform}(0,1)\\
\delta_{id} &\sim \text{log-Gaussian}\left(\mu_d^\delta, \tfrac{1}{(\sigma^\delta)^2}\right)\\
\mu_d^\kappa &\sim \text{Gaussian}(0,1)\\
\sigma^\kappa &\sim \text{uniform}(0,4)\\
\kappa_{id} &\sim \text{log-Gaussian}\left(\mu_d^\kappa, \tfrac{1}{(\sigma^\kappa)^2}\right)\\
\mu_{ia}^\omega &\sim \text{Gaussian}(0,1)\\
\gamma_{ia}^\omega &\sim \text{Gaussian}(0,1)\\
\frac{\omega_{ic}}{1-\omega_{ic}} &= \begin{cases} \exp\left(\mu_{ia}^\omega + \frac{\gamma_{ia}^\omega}{2}\right) & \text{if } c > 0\\ \exp\left(\mu_{ia}^\omega - \frac{\gamma_{ia}^\omega}{2}\right) & \text{if } c < 0\\ \exp\left(\mu_{ia}^\omega\right) & \text{if } c = 0\end{cases}\\
z_{isdct} &\sim \text{Bernoulli}\left(\omega_{ic}\right)\\
\beta_i &\sim \text{uniform}\left(0,1\right)\\
\theta_{isdct} &\sim \begin{cases} \text{Gaussian}\left(\phi_{isdct}, \kappa_{id}\right) & \text{if } z_{isdct} = 0\\ \text{Gaussian}\left(q_{isdct}, \beta_i\kappa_{id}\right) & \text{if } z_{isdct} = 1\end{cases}\\
\boldsymbol{y}_{isdct} &\sim \text{CDDM}_\circ\left(\delta_{id}, \eta_{is}, \tau_i, \text{mod}(\theta_{isdct}, 2\pi)\right)
\end{aligned}
$$

Fig. 7 Graphical model for the reanalysis of cued orientation judgments from Kvam (2019)

ary radius, and nondecision time. One way to interpret these assumptions is as models of cross-trial variability in the CDDM parameters, illustrating that graphical models can provide a flexible and practical alternative to integrating variability assumptions directly into the likelihood function itself (Zhou et al., 2021, 2023).

Drift Angle

The drift angle θ_{isdct} is represented by an unshaded node because it is latent. We assume that there are two qualitatively different possibilities for the drift angle on each trial.[4] It can either be based on the mean orientation of the presented stimuli, or on the cue. These two possibilities are ϕ_{isdct} and q_{isdct}, which are known properties of the trial, and hence represented by shaded nodes.

Which value θ_{iscdt} takes is determined by a latent binary indicator z_{isdct}, represented by a square node because it is discrete. Formally,

$$\theta_{isdct} \sim \begin{cases} \text{Gaussian}\left(\phi_{isdct}, \tau_{id}^\theta\right) & \text{if } z_{isdct} = 0\\ \text{Gaussian}\left(q_{isdct}, \beta_i\tau_{id}^\theta\right) & \text{if } z_{isdct} = 1.\end{cases} \tag{6}$$

The binary indicator follows a Bernoulli distribution with a base rate that depends on the participant and the cue deflection

$$z_{iscdt} \sim \text{Bernoulli}\left(\omega_{ic}\right). \tag{7}$$

The base rate with which participant i uses cues with deflection c is assumed to be ω_{ic}.

Since our research goals include testing whether ω_{ic} changes for positive versus negative cue deflections with the same magnitude, we define

$$\frac{\omega_{ic}}{1-\omega_{ic}} = \begin{cases} \exp\left(\mu_{ia}^\omega + \gamma_{ia}^\omega/2\right) & \text{if } c > 0\\ \exp\left(\mu_{ia}^\omega - \gamma_{ia}^\omega/2\right) & \text{if } c < 0\\ \exp\left(\mu_{ia}^\omega\right) & \text{if } c = 0.\end{cases} \tag{8}$$

These definitions mean that μ_{ia}^ω controls the bias on the logit scale towards using the cue or stimulus information for deflection magnitude a, while γ_{ia}^ω is an effect size on the

[4] Other assumptions are possible, such as drift angle being some weighted combination of cue and stimulus information. While these more complicated possibilities could certainly be implemented, we consider just the simplest case in which the drift angle is determined by one or the other.

logit scale between positive and negative deflections of the same magnitude. This part of the graphical model provides an example of creating a structure to test research hypotheses. In particular, comparing the prior and posterior on the log effect size γ_{ia}^{ω} provides a principled way to estimate Bayes factors testing whether or not participants have different base rates for positive versus negative cue deflections with the same magnitude.

Depending on whether the stimulus or the cue is used, different precisions apply to how accurately the drift angle follows this information. These precisions are represented by the parameters τ_{id}^{θ} and β_i. We assume that there are individual differences in stimulus information precision that depend on the stimulus difficulty. For person i in difficulty condition d,

$$\tau_{id}^{\theta} \sim \text{log-Gaussian}\left(\mu_d^{\tau^\theta}, \frac{1}{\left(\sigma^{\tau^\theta}\right)^2}\right) \tag{9}$$

with priors on the mean and standard deviation that define the Gaussian distribution of individual differences:

$$\mu_d^{\tau^\theta} \sim \text{Gaussian}(0, 1) \tag{10}$$

$$\sigma^{\tau^\theta} \sim \text{uniform}(0, 4). \tag{11}$$

Note that the assumption is that the mean changes with stimulus difficulty, but the variability of individual differences is the same for all of the different levels of stimulus difficulty.

The cue information has a precision that is proportional to that of the stimulus information for the trial depending on each participant. This requires defining the constant of proportionality β_i for person i as

$$\beta_i \sim \text{uniform}(0, 1). \tag{12}$$

This means that the variability of the information provided by the cue distribution is always equal or greater to the stimulus one.

Drift Length

We assume there are individual differences in the drift lengths δ_{id} that depend on stimulus difficulty. For person i in difficulty level d

$$\delta_{id} \sim \text{log-Gaussian}\left(\mu_d^{\delta}, \frac{1}{\left(\sigma^{\delta}\right)^2}\right). \tag{13}$$

with priors

$$\mu_d^{\delta} \sim \text{Gaussian}(0, 1) \tag{14}$$

$$\sigma^{\delta} \sim \text{uniform}(0, 1). \tag{15}$$

As was the case for the base rate of cue versus stimulus use, we assume that only the mean changes with stimulus difficulty, but the variability of individual differences is the same.

Boundary Radius

The boundary radius η_{is} is assumed to be independent across both participants and speed-accuracy conditions. In order to test whether speed-accuracy instructions affect a participant's boundary radius, η_{is} is defined in the model in terms of the mean boundary radius on the log scale μ_i^{η} for participant i over both conditions and the effect size difference on the log scale γ_i^{η}. This leads to the following definitions:

$$\eta_{is} = \begin{cases} \exp\left(\mu_i^{\eta} + \gamma_i^{\eta}/2\right) \text{ if } s = \text{accuracy} \\ \exp\left(\mu_i^{\eta} - \gamma_i^{\eta}/2\right) \text{ if } s = \text{speed}\,. \end{cases} \tag{16}$$

This part of the graphical model provides a second example of creating a structure to test research hypotheses. In particular, comparing the prior and posterior on the log effect size γ_i^{η} provides a principled way to estimate Bayes factors testing whether or not participants use different boundaries in speed versus accuracy conditions.

Nondecision Time

Finally, nondecision time does not have any additional model structure, and each participant is independently given the prior

$$\tau_i \sim \text{uniform}(0, \min y_{i1}), \tag{17}$$

where $\min y_{i1}$ represents the minimum response time for participant i over all trials.

Results

The results of analyses addressing the four research questions are presented in the four panels of Fig. 8. They are based on the computational approximation to the joint posterior distribution of the model provided by JAGS. This approximation is based on four chains with 5000 recorded samples after 45000 discarded burn-in samples. Once again, we only considered convergent chains with $\hat{R} < 1.05$.

To evaluate the descriptive adequacy of our model, we conducted a posterior predictive check (Baribault & Collins, 2023; Lee, 2018). We compared the joint posterior predictive distribution of error in the decision angle and response time to the observed data. We did these comparisons separately for each of the six participants for both speed and accuracy instructions for each level of stimulus difficulty and each type

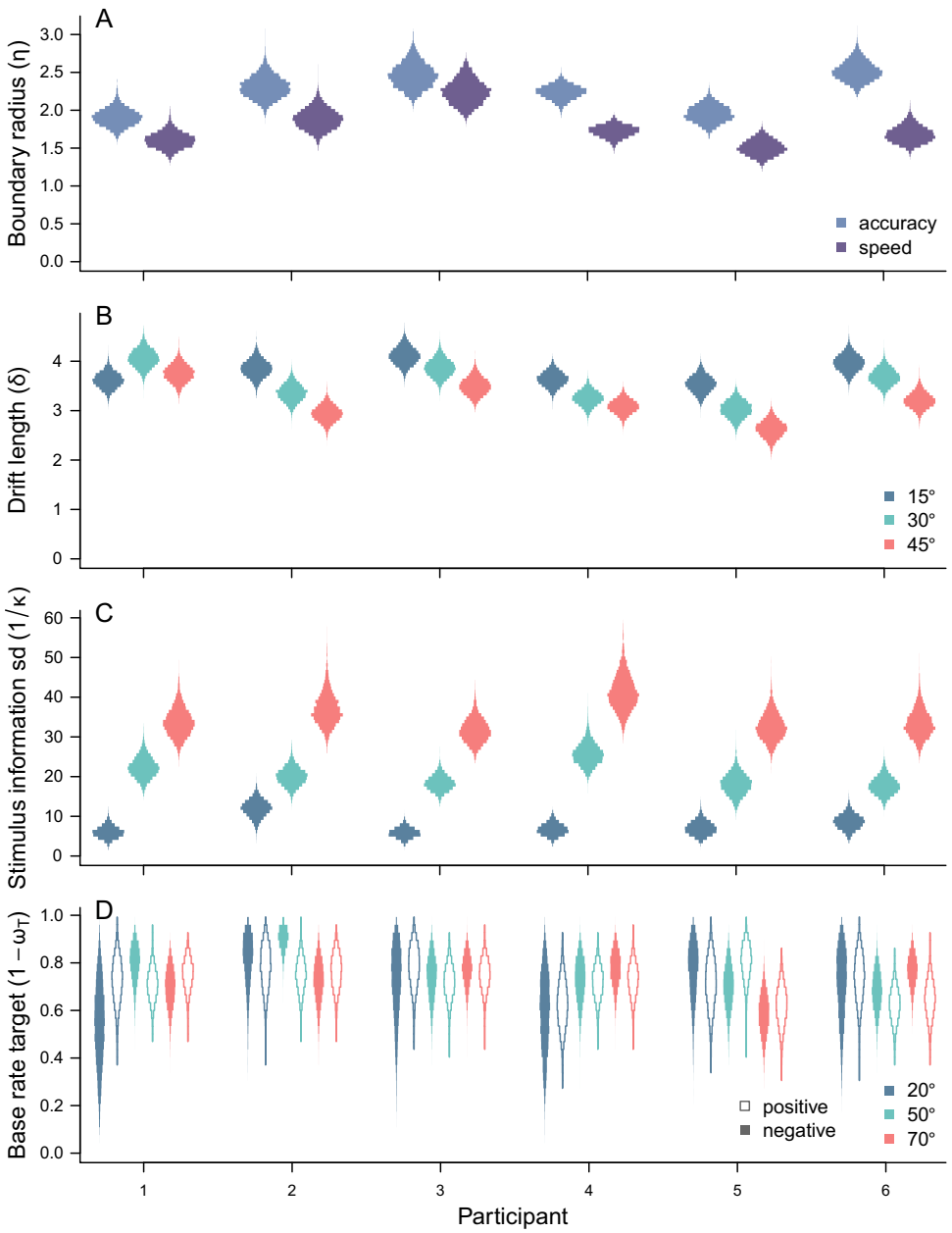

Fig. 8 Posterior distributions of the parameters of interest, with parameter values on the y-axis and participants on the x-axis. **A** shows the boundary radius parameter η for the accuracy (blue) and speed (purple) conditions. **B** shows the drift length parameter δ for each difficulty condition, 15 (blue) 30 (green), and 45° (orange). **C** shows the standard deviation of the drift angle $1/\sqrt{\tau^{\theta}}$ for each difficulty condition. **D** shows the mixing probability ϕ for the 20° (blue), 50 (green), and 70 (orange) cue deflection conditions. Filled histograms indicate negative (negative) deflection trials

of cue. All of these analyses are available in the supplementary information. The vast majority of the observed decisions and response times were in high-density regions of the posterior predictive distribution. The only potential systematic failures of descriptive adequacy occurred in relation to difficult stimuli, which sometimes led to responses that were well described in terms of the decision angle, but with longer response times than the model expects. This weakness of the model could likely be addressed by allowing for contaminant response strategies, such as the delayed startup sometimes used in standard drift-diffusion model (Vandekerckhove & Tuerlinckx, 2007; Vandekerckhove et al., 2011). Because the poorly described data were very rare, we did not implement additional response strategies, and regard the current model as descriptively adequate for the research questions it was designed to answer.

The first research question about differences in caution is addressed by Fig. 8A. The panel shows the posterior samples of the boundary radius parameters η_{is} for each participant in both speed and accuracy conditions. For most of the participants, it is clear that the posterior distribution of the parameter for the accuracy conditions is higher. The η column of Table 1 confirms this result in terms of Bayes factors comparing the order-restricted alternative hypothesis that the accuracy condition boundary radius is greater to the null hypothesis that the boundaries are the same. These Bayes factors

are approximated using the Savage-Dickey method (Wetzels et al., 2010). For every participant except participant 3 the Bayes factor is greater than 1000 in favor of the hypothesis that the boundary radius is higher for accuracy trials.

The second research question about the speed of information processing and task difficulty is addressed by Fig. 8B. The panel shows the posterior distribution of the drift length δ_{id} for each participant and task difficulty. It is clear that the order constraints are followed by all of the participants except for participant 1. The δ columns of Table 1 confirm this result in terms of the posterior probability that the drift lengths satisfy the order constraint. For participant 1, the posterior probability of the order constraints is close to 0, however, for the rest of the participants it is higher than 0.8.

The third research question about the consistency of information and task difficulty is addressed by Fig. 8C. The panel shows the posterior distributions of the standard deviation of stimulus information $1/\sqrt{\tau^\theta}$ for each participant and task difficulty. It is clear the order constraint is followed by all six participants. The σ column of Table 1 confirms this result in terms of the posterior probability that the standard deviations satisfy the order constraint. The posterior probability of the order constraints is close to 1 for all participants.

The final research question about whether positive and negative deflections have different impacts on cue use is addressed by Fig. 8D. The panel shows the posterior distribution of the base rate of stimulus used for each participant and the deflection angle. The values of the base rate show that participants generally used the stimulus information in the majority of trials. Comparing the positive (unfilled) and negative (filled) deflections of the same magnitude suggests the base rates are often similar. The Bayes factors testing for the sameness or difference of the base rates are presented in the ω columns of Table 1, expressed in terms of evidence for a difference. Most of the Bayes factors are close to one, indicating there is not clear evidence in favor of either hypothesis. This provides an example of the ability to use Bayes factors with the CDDM not only to find evidence for sameness (the null) or a difference (the alternative), but also to fail to find clear evidence for either. The obvious conclusion is that more data are needed to address this research question.

Discussion

Our application to modeling orientation judgments highlights the usefulness of the JAGS implementation of the CDDM. Graphical models provide a high-level language for probabilistic psychological models for constructing tailored CDDM models that deal with circular decisions and response times. The graphical model we developed has the CDDM at its core, predicting behavior on each trial, but makes assumptions about how model parameters change over trials, stimuli, and people that are specific to the experimental design that generated the data and the motivating research questions.

As argued by Lee (2011, 2018), there are two complementary features of this approach. One feature is that graphical models afford significant freedom and flexibility in model development. A wide range of theoretical assumptions can be implemented, tested, and used. The model of orientation judgments we developed made extensive use of hierarchical and latent-mixture structures, which allowed for more theory to be incorporated. For example, instead of treating the drift angle as a free parameter to be estimated, our model formalized the idea that people could use either cue or stimulus information, that this choice could depend on the deflection between the cue and stimulus, and that direction information was perceived differently by different participants. Existing applications of the CDDM have proposed other sorts of mixture accounts of people's decision making, such as responses in a lexical decision task being based on the target word, intrusions, or guessing (Zhou et al., 2023). These have been modeled in terms of the proportions of each response time at an aggregate level. The graphical modeling approach to latent mixtures we have demonstrated would allow inferences about response types to be made at the level of individual trials. This additional level of modeling detail would be especially important if modeling goals extended

Table 1 Bayes factors and posterior probabilities of order constraints addressing the four research questions

Participant	Bayes factors				Posterior probabilities	
	η	$\omega_{\pm 20}$	$\omega_{\pm 50}$	$\omega_{\pm 70}$	$\delta_{15} > \delta_{30} > \delta_{45}$	$\sigma_{15} < \sigma_{30} < \sigma_{45}$
1	> 1000	1.083	2.083	2.225	0.054	0.992
2	> 1000	1.107	19.175	1.711	0.997	0.999
3	13	1.046	1.178	2.291	0.952	0.999
4	> 1000	1.063	1.067	2.100	0.917	0.999
5	> 1000	0.975	1.713	1.668	0.994	0.999
6	> 1000	3.027	1.164	2.096	0.965	0.999

beyond treating trials as independently and identically distributed and considered the possibility of sequential effects, adaptation, or any other sort of non-stationarity. Overall, the goal of psychological modeling is to develop accounts that are as general and complete as possible, and graphical models provide the ability to propose ambitious accounts of people's behavior.

The second noteworthy feature of graphical modeling is that theoretical freedom is complemented by methodological rigor. Whatever model is proposed, its contact with data is governed by Bayesian inference, which by virtue of following the laws of probability is complete, consistent, and coherent (Cox, 1961; Jaynes, 2003). We think that the use of posterior distributions and Bayes factors improves on the use of maximum likelihood estimates and the Akaike Information Criterion and Bayesian Information Criterion in existing applications of the CDDM (e.g., Smith et al., 2020; Zhou et al., 2021). Most generally, the rigor of Bayesian inference means that CDDM modeling can be evaluated against data in a way that acknowledges uncertainty and provides a safeguard against overly ambitious models that overfit the data (Pitt et al., 2002).

Our application to orientation judgments used Bayes factors to find evidence for a null hypothesis regarding the direction of deflections, which is an example of how Bayesian evaluation can lead to a proposed model being rejected and a psychologically simpler model being preferred. Our application also provided examples in which model assumptions were justified using quantified evidence provided by the data. One example was the Bayes factor for the difference between boundaries for speed and accuracy conditions. Another was the probability of order constraints relating drift rates to different types of stimuli.

Beyond hierarchical and latent-mixture structures, graphical modeling in JAGS offers a number of other possibilities not demonstrated in our application. One possibility, discussed by Smith et al. (2020), is to use informative prior distributions to model categorical perception. Implementing this sort of model, in which theoretical assumptions are naturally represented in parameter priors rather than likelihood functions (Vanpaemel & Lee, 2012), requires a fully Bayesian formulation of a CDDM model.

A second possibility is what Lee (2011, 2018) calls common-cause modeling, in which the same psychological variable is assumed to influence behavior observed in multiple contexts. This idea is the basis for well-developed joint models of behavioral and neural data, which are often implemented in JAGS (Turner et al., 2019). The common cause idea, however, applies equally well for linking multiple sources of behavioral data. For example, the individual differences in how participants use the cue or stimulus for direction information in the current orientation judgment task may be related to their behavior in other perceptual attention tasks. Constructing a graphical model that formalizes this possibility is straightforward, requiring a graph structure in which the same parameter or parameters play a role in generating both sets of data (e.g., Guan & Lee 2018; Guan et al., 2020; Vandekerckhove, 2014; Oravecz & Vandekerckhove, 2020).

A final possibility for future applications involves the extension to categorical decision boundaries discussed by Smith (2016). Within JAGS this could be achieved by censoring using the `dinterval` distribution, which implements situations in which continuous quantities are only observed in terms of discrete outcomes. Two examples are shown in Fig. 9, highlighting how two of our motivating circular decisions in Fig. 1 involve discrete decisions. In the left panel, the choice options for choosing the color of a shirt are a set of color words. In the right panel, the direction of the voice is indicated by naming the person speaking. To model these sorts of discrete decisions, the continuous location on the circular boundary of the CDDM must be censored according to choice boundaries. JAGS provides a censoring capability directly through its `dinterval` distribution.

A third possibility is the application of CDDMs to decisions that are semi-circular in nature. That is, where there is a continuum of possible decisions corresponding to points on a semi-circle, along with a similarity relationship between the

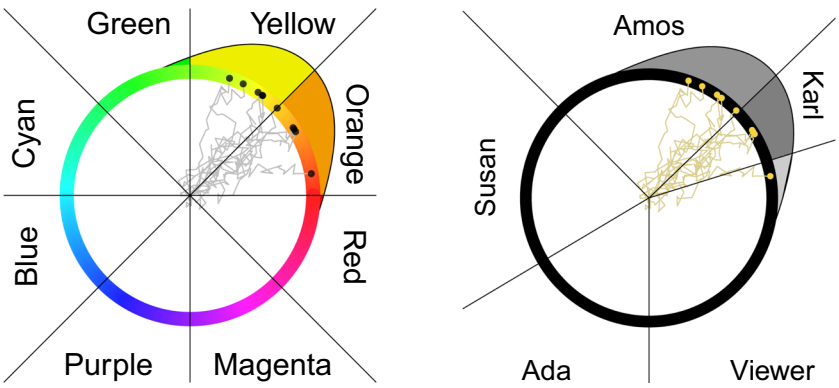

Fig. 9 Categorical-choice extensions of the CDDM. The left panel considers the color identification situation in Fig. 1 for a task in which the choice options are color words. The right panel considers the voice direction situation for a task in which the choice options are the names of the possible speakers

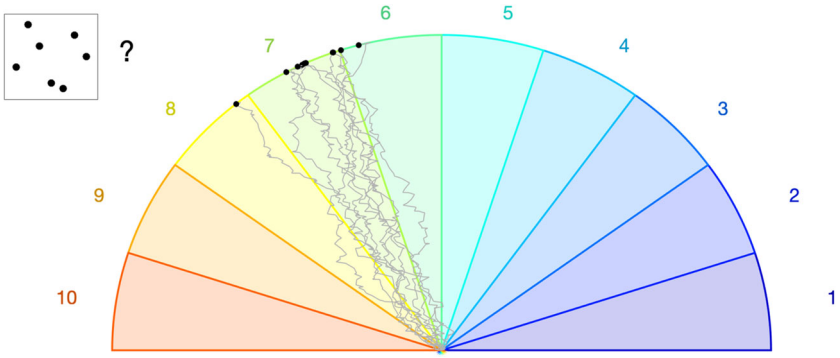

Fig. 10 A categorical-choice extension of the CDDM to mathematical problems with answers that are naturally represented on a semi-circle

decision alternatives. The difference from a classical circular decision structure is that the end points of the decisions have the lowest degree of similarity. One concrete example, shown in Fig. 10 involves mathematical problem solving where the answers lie on a number line that may be represented as points on a semi-circle (e.g., Mistry et al., 2023).

Conclusion

Sequential sampling models, and especially the drift-diffusion model, are the most successful and widely used models of the time course of human decision making. These models are capable of making predictions about both the choices people make and the time it takes them to make these choices. Most applications have considered forced-choice two-alternative decision tasks, consistent with a model architecture in which an evidence tally accumulates over time towards one of two boundaries. More recently, the development of model architectures that allow many evidence tallies to accumulate towards many boundaries has led to applications to tasks involving multi-alternative choice. These models assume, however, that there is a finite set of nominally-scaled choice alternatives. The CDDM extends the scope of sequential sampling models to allow for choice and response time modeling in situations where there is a continuum of choices that can be represented on a circle. In this way, the CDDM opens up many new possibilities for modeling the time course of human decision making.

An important part of realizing the promise of the CDDM is to allow it to be used as the key component of models tailored to specific tasks and data, and designed to answer specific research questions. Embedding the CDDM within a graphical modeling framework is one way to achieve this, because it allows the development of very general probabilistic generative models of psychological processes, and facilitates fully Bayesian inference via computational methods. We implemented the CDDM as a module within the JAGS graphical modeling language and demonstrated the accuracy of our implementation. We then demonstrated, in an application to orientation judgments, how the CDDM can be used to develop an account of task behavior that captures assumptions about individual differences across stimulus and task conditions and can provide parameter inferences and model comparisons that address research questions. We hope this application serves as an example of how the CDDM can be used to model and understand new research questions involving the time course of human decision making.

Author Contributions AFCP and JV developed the JAGS module. MV and MDL led the development of the graphical modeling application. All authors contributed to the interpretation of results and writing the paper.

Funding MV, AFCP, PKM, VM, and MDL were supported by National Science Foundation grant #2024856. AFCP and JV were supported by National Science Foundation grants #1230118, #1658303, #1850849, and #2051186.

Availability of Data and Materials The data set from Kvam (2019) is available on the Open Science Framework at https://osf.io/px274/.

Code Availability The **jags-cddm** module is available at https://github.com/joachimvandekerckhove/jags-cddm. Code for the application is available at https://github.com/ManuelVU/application-jags-cddm.

Declarations

Ethics Approval This study involves the use of previously published data from Kvam (2019).

Consent to Participate Not applicable

Consent for Publication Not applicable

Conflict of Interest The authors declare no competing interests.

References

Baribault, B., & Collins, A. G. E. (2023). Troubleshooting Bayesian cognitive models. *Psychological Methods*. https://doi.org/10.1037/met0000554

Cox, R. T. (1961). *The algebra of probable inference*. Baltimore, MD: Johns Hopkins University Press. https://doi.org/10.56021/9780801869822.

Gelman, A., Carlin, J. B., Stern, H. S., Dunson, D. B., Vehtari, A., & Rubin, D. B. (2013). *Bayesian data analysis*. USA, New York: Taylor & Francis, 3rd edition. https://doi.org/10.1201/b16018.

Guan, M., & Lee, M. D. (2018). The effects of goals and environments on human performance in optimal stopping problems. *Decision, 5*(4), 339–361. https://doi.org/10.1037/dec0000081

Guan, M., Stokes, R., Vandekerckhove, J., & Lee, M. D. (2020). A cognitive modeling analysis of risk in sequential choice tasks. *Judgment and Decision Making, 15*(5), 823–850. https://doi.org/10.1017/S1930297500007956

Jaynes, E. T. (2003). *Probability theory: The logic of science*. Cambridge, UK: Cambridge University Press. https://doi.org/10.1017/CBO9780511790423

Kvam, P. D. (2019). Modeling accuracy, response time, and bias in continuous orientation judgements. *Journal of Experimental Psychology: Human Perception and Performance, 45*(3), 301–318. https://doi.org/10.1037/xhp0000606

Lee, M. D. (2018). Bayesian methods in cognitive modeling. In J. Wixted & E.-J. Wagenmakers (Eds.), *The Stevens' Handbook of Experimental Psychology and Cognitive Neuroscience. Volume 5: Methodology* chapter 2, (pp. 37–84). John Wiley & Sons, 4th edition. https://doi.org/10.1002/9781119170174.epcn502.

Lee, M. D. (2011). How cognitive modeling can benefit from hierarchical Bayesian models. *Journal of Mathematical Psychology, 55*(1), 1–7. https://doi.org/10.1016/j.jmp.2010.08.013

Lee, M. D., & Wagenmakers, E.-J. (2013). *Bayesian cognitive modeling: A practical course*. Cambridge: Cambridge University Press. https://doi.org/10.1017/CBO9781139087759

Mistry, P. K., Strock, A., Liu, R., Young, G., & Menon, V. (2023). Learning-induced reorganization of number neurons and emergence of numerical representations in a biologically inspired neural network. *Nature Communications, 14*, 1–21. https://doi.org/10.1038/s41467-023-39548-5

Oravecz, Z., & Vandekerckhove, J. (2020). A joint process model of consensus and longitudinal dynamics. *Journal of Mathematical Psychology, 98*, 1–8. https://doi.org/10.1016/j.jmp.2020.102386

Pitt, M. A., Myung, I. J., & Zhang, S. (2002). Toward a method of selecting among computational models of cognition. *Psychological Review, 109*(3), 472–491. https://doi.org/10.1037/0033-295x.109.3.472

Plummer, M. (2003). JAGS: A program for analysis of Bayesian graphical models using Gibbs sampling. In K. Hornik, F. Leisch, & A. Zeileis (Eds.), *Proceedings of the 3rd International Workshop on Distributed Statistical Computing*, volume 124 (pp. 1–10). Vienna, Austria: (DSC 2003). https://www.r-project.org/conferences/DSC-2003/Proceedings/Plummer.pdf.

Qarehdaghi, H. & Rad, J. A. (2022). *EZ-CDM for modeling continuous decisions by everyone! Fast, simple, robust, and accurate estimation of circular diffusion model parameters*. https://doi.org/10.31234/osf.io/rzqhg.

Ratcliff, R. (1978). A theory of memory retrieval. *Psychological Review, 85*(2), 59–108. https://doi.org/10.1037/0033-295x.85.2.59

Ratcliff, R., & McKoon, G. (2008). The diffusion decision model: Theory and data for two-choice decision tasks. *Neural Computation, 20*(4), 873–922. https://doi.org/10.1162/neco.2008.12-06-420

Selker, R. (2016). *JAGS ExGauss module*. https://github.com/raviselker/jags-exgauss.

Selker, R. (2018a). *JAGS module template*. https://github.com/raviselker/jags-moduleTemplate.

Selker, R. (2018b). *JAGS RescorlaWagner module*. https://github.com/raviselker/jags-rescorlaWagner.

Smith, P. L. (2016). Diffusion theory of decision making in continuous report. *Psychological Review, 123*(4), 425–451. https://doi.org/10.1037/rev0000023

Smith, P. L., & Corbett, E. A. (2019). Speeded multielement decision-making as diffusion in a hypersphere: Theory and application to double-target detection. *Psychonomic Bulletin & Review, 26*(1), 127–162. https://doi.org/10.3758/s13423-018-1491-0

Smith, P. L., Garrett, P. M., & Zhou, J. (2023). Obtaining stable predicted distributions of response times and decision outcomes for the circular diffusion model. *Computational Brain & Behavior, Advance online publication,*. https://doi.org/10.1007/s42113-023-00174-5

Smith, P. L., Saber, S., Corbett, E. A., & Lilburn, S. D. (2020). Modeling continuous outcome color decisions with the circular diffusion model: Metric and categorical properties. *Psychological Review, 127*(4), 562–590. https://doi.org/10.1037/rev0000185

Turner, B. M., Forstmann, B. U., & Steyvers, M. (2019). A tutorial on joint modeling. In *Joint models of neural and behavioral data* (pp. 13–37). Cham: Springer International Publishing. https://doi.org/10.1007/978-3-030-03688-1_2.

Vandekerckhove, J. (2014). A cognitive latent variable model for the simultaneous analysis of behavioral and personality data. *Journal of Mathematical Psychology, 60*, 58–71. https://doi.org/10.1016/j.jmp.2014.06.004

Vandekerckhove, J., & Tuerlinckx, F. (2007). Fitting the Ratcliff diffusion model to experimental data. *Psychonomic Bulletin & Review, 14*(6), 1011–1026. https://doi.org/10.3758/BF03193087

Vandekerckhove, J., Tuerlinckx, F., & Lee, M. D. (2011). Hierarchical diffusion models for two-choice response time. *Psychological Methods, 16*(1), 44–62. https://doi.org/10.1037/a0021765

Vanpaemel, W., & Lee, M. D. (2012). Using priors to formalize theory: Optimal attention and the generalized context model. *Psychonomic Bulletin & Review, 19*, 1047–1056. https://doi.org/10.3758/s13423-012-0300-4

Wabersich, D. (2016a). *Jags Amoroso module*. https://github.com/yeagle/jags-amoroso.

Wabersich, D. (2016b). *Jags VonMises module*. https://github.com/yeagle/jags-vonmises.

Wabersich, D. (2018). *Jags Wiener module*. https://github.com/yeagle/jags-wiener.

Wabersich, D., & Vandekerckhove, J. (2014). Extending JAGS: A tutorial on adding custom distributions to JAGS (with a diffusion model example). *Behavior Research Methods, 46*, 15–28. https://doi.org/10.3758/s13428-013-0369-3

Wetzels, R., Grasman, R. P. P. P., & Wagenmakers, E. (2010). An encompassing prior generalization of the Savage-Dickey density ratio test. *Computational Statistics and Data Analysis, 54*(9), 2094–2102. https://doi.org/10.1016/j.csda.2010.03.016

Zhou, J., Osth, A. F., Lilburn, S. D., & Smith, P. L. (2021). A circular diffusion model of continuous-outcome source memory retrieval: Contrasting continuous and threshold accounts. *Psychonomic Bulletin & Review, 28*(4), 1112–1130. https://doi.org/10.3758/s13423-020-01862-0

Zhou, J., Osth, A. F., & Smith, P. L. (2023). The spatiotemporal gradient of intrusion errors in continuous outcome source memory: Source retrieval is affected by both guessing and intrusions. *Cognitive Psychology, 141*(101552), 1–28. https://doi.org/10.1016/j.cogpsych.2023.101552

Publisher's Note Springer Nature remains neutral with regard to jurisdictional claims in published maps and institutional affiliations.

Springer Nature or its licensor (e.g. a society or other partner) holds exclusive rights to this article under a publishing agreement with the author(s) or other rightsholder(s); author self-archiving of the accepted manuscript version of this article is solely governed by the terms of such publishing agreement and applicable law.